ARTICLE

DOI: 10.1590/2317-4889201920190019

BJGEO Brazilian Journal of Geology

Integrating geological and airborne geophysical data to review the cartography of Rio Itanguá Batholith, Araçuaí Orogen, Brazil

Julia Grochowski[1,2]*, Matheus Kuchenbecker[1,2,3], Danilo Barbuena[1,2], Tiago Amâncio Novo[3]

ABSTRACT

Rio Itanguá Batholith (RIB) is a plutonic body located in the Northern border of Guanhães block, one of the various basement blocks reworked within the Araçuaí orogen, Eastern Brazil. Although its existence is known since the beginning of the 20th century, its tectonic history remains poorly understood. The RIB was mapped at 1:100,000 scale in the 1990s, before geophysical and satellite data became available. This work aims to re-evaluate the cartography of the RIB, as an initial step towards understanding its genesis and evolution. In order to do so, field and petrographic data, together with airborne gamma-ray spectrometry and magnetometry data, were integrated, resulting in a geologic map that shows different features from the previous maps produced in the area, such as the batholith division into two different petrographic and geophysical units; the presence of a mafic dike intruding the batholith rocks and the reduction in size of the batholith area. The magnetometric and gamma-spectrometric data proved to be important tools for geological mapping, and the substantial data obtained in the analysis of this tiny area points to the importance of re-evaluating older geological maps, taking geophysical data into account.

KEYWORDS: Rio Itanguá Batholith; Geological mapping; Gamma-ray spectrometry; Magnetometry; Guanhães Block; Araçuaí Orogen.

INTRODUCTION

Geological mapping is one of the most important assignments of geologists in the modern society. It is essential to the exploration of mineral resources and to planning and management of land use, in urban or rural environments. As a scientific activity, geological mapping provides information of the spatial distribution of units and nature of boundaries between rock bodies, which is indispensable to establish the timeline of events that composes a region geological history. Furthermore, it is during detailed geological mapping that the geologists find key rock outcrops, suitable for modern laboratory analysis that provide information of the age and physicochemical evolution of our planet.

Since the first geological maps were published (*e.g.*, Cuvier & Brongniart 1811, Smith 1815), the development of technology and methods involved in the mapping process have gone through a huge revolution. The means of transportation advanced from horseback to four-wheel drive vehicles, and the methods of data collection and presentation were strongly improved by the advent of global positioning systems (GPS), geographic information systems (GIS), and satellite imagery (*e.g.*, Whitmeyer *et al.* 2010). These advances were further improved by the development of airborne geophysical acquisition — notably magnetometry and gamma-ray spectrometry — , which provided a continuous and objective dataset across large areas, where geological outcrop information may be discontinuous and, sometimes, subjective (Rattenbury *et al.* 2016). This is especially relevant for the mapping of tropical regions, in which dense forests and intense chemical weathering result in large areas with scarce rock outcrops.

Airborne geophysical data have been widely used as a tool for the interpretation of geological features, aiding geological mapping efforts and mineral prospecting projects (*e.g.*, Rattenbury *et al.* 2016, Barbuena *et al.* 2013, Reis *et al.* 2012, Amaral & Santos 2008). Hence, magnetometry and gamma-ray spectrometry data can be combined with field data in order to better define the limits of geological units, according to their unique characteristics, as well as to mark structural features.

One of the most important mineral areas in Brazil is Minas Gerais State, which hosts historical gold and iron deposits that have been mined since the 17th century. Due to the importance

Supplementary material

Supplementary data associated with this article can be found in the online version: Supplementary Table 1

[1]Programa de Pós-Graduação em Geologia, Centro de Estudos em Geociências, Instituto de Ciência e Tecnologia, Universidade Federal dos Vales do Jequitinhonha e Mucuri – Diamantina (MG), Brazil. E-mails: juliagrochowski@hotmail.com; mk.geologia@gmail.com; danilo.barbuena@ict.ufvjm.edu.br

[2]Laboratório de Estudos Tectônicos, Centro de Estudos em Geociências, Instituto de Ciência e Tecnologia, Universidade Federal dos Vales do Jequitinhonha e Mucuri – Diamantina (MG), Brazil.

[3]Centro de Pesquisas Professor Manoel Teixeira da Costa, Instituto de Geociências, Universidade Federal de Minas Gerais, Campus Pampulha – Belo Horizonte (MG), Brazil. E-mail: tiagoanovo@gmail.com

*Corresponding author.

© 2019 The autors. This is an open access article distributed under the terms of the Creative Commons license.

of their mineral resources, several areas in Minas Gerais underwent systematic geological mapping since the first half of the 20th century. In the 1990s, the state government started an important geological mapping effort at 1:100.000 scale in partnership with the Universidade Federal de Minas Gerais (UFMG), which begun in areas around the Espinhaço ridge, in the so-called Espinhaço Project (Grossi-Sad *et al.* 1997a). Since then, after several mapping projects carried out by three institutions (CODEMIG, CPMTC/UFMG, CPRM), Minas Gerais state was completely covered by 1:100,000 geological maps. Within the Espinhaço Project, the areas were mapped mainly by using black-and-white aerial photographs of the 1960s, which supported the fieldworks and drawing of geological boundaries. The resulting maps prompted great advances in the geological research and have been the state-of-the-art of geological cartography of the region since then.

Between 2001 and 2013, the Economic Development Company of Minas Gerais (CODEMIG) carried out an airborne geophysical survey of the state. When the results became available, reassessing the previously mapped areas using magnetometry and gamma-ray spectrometry data became possible. In this context, this work aims to re-evaluate the cartography of Rio Itanguá Batholith (RIB), which is one of the various basement plutonic bodies mapped within the Espinhaço Project, by using airborne geophysical and new field data. Basement complexes are tectonic "black boxes", invariably registering all the tectonic events that occurred in a region. Although fairly studied in the past (*e.g.*, Hettich 1973, Toloczyki 1982), the RIB has few information concerning its age and geotectonic context. An accurate evaluation of its limits, therefore, is an initial step towards understanding the genesis and evolution of the RIB itself and the deformational and metamorphic events that affected the RIB and its vicinity, which are not always detectable on younger sedimentary units.

GEOLOGICAL CONTEXT

The RIB is an igneous body located in the Central-Eastern part of Minas Gerais state, Brazil, nearby the cities of Felício dos Santos and Senador Modestino Gonçalves. It was first mentioned in the literature by Moraes (1937), referred to as the Mercês granite in this classic work. Later in the 1970s and 1980s, it was studied by Gorlt (1972), Hettich (1973) and Toloczyki (1982). It was in the late 1990s that the RIB got its current denomination, due to the river that runs through its oriental border, the Itanguá river. It was then mapped at 1:100,000 scale in the Carbonita and Rio Vermelho geological maps of the Espinhaço Project (Grossi-Sad *et al.* 1997b, Souza & Grossi-Sad 1997).

Tectonically, the RIB is located within the limits of Araçuaí orogen, which covers a large area extending from the Eastern border of São Francisco craton to the Atlantic Ocean (*e.g.* Almeida 1977, Pedrosa-Soares *et al.* 2007, Alkmin 2017). The Araçuaí Orogen is a confined orogen formed during the amalgamation of Western Gondwana in the Neoprotorozoic/Cambrian boundary. It comprises several tectonic components, such as passive margin sediments, ophiolites, suture zone, magmatic arcs, and pre- and post-collisional plutons (Pedrosa-Soares *et al.* 2007).

Within the Araçuaí orogen, some basement blocks were reworked during the orogeny. The biggest and southernmost block, known as Guanhães block, is composed by Archean (mostly tonalite-trondhjemite-granodiorite (TTG) and metasedimentary sequences) and Paleoproterozoic (plutonic and metasedimentary sequences) units. The RIB is located at the Northern part of Guanhães block (Fig. 1) and is surrounded by rocks of Neoproterozoic Macaúbas Group, which records rift and passive margin sequences that precede the orogeny (*e.g.*, Kuchenbecker *et al.* 2015).

The RIB is mapped as an approximately rectangular igneous body, in map view (Fig. 1). It is composed of medium-grained equigranular to porphyritic granitoids — petrographic varieties including granite, granodiorite, and tonalite. These rocks are commonly affected by shear zones, both in the borders and center of the batholith, and can show anastomosing foliation as a result of shear deformation (Grossi-Sad *et al.* 1997b). The main lithofacies described is a two-mica leucogranite, with or without feldspar phenocrysts and with titanite and allanite as common accessory phases (Grossi-Sad *et al.* 1997b, Souza e Grossi-Sad 1997, Toloczyki 1982, Hettich 1973). As indicated by Pinto & Silva (2014) in the last Minas Gerais geological map, the presumed crystallization age for the RIB is Paleoproterozoic, based on preliminary geochronological data obtained by Brito Neves *et al.* (1979) and Hagedorn (2004), but the unit still lacks precise dating.

The batholith is almost entirely surrounded by the rocks of Macaúbas Group through erosive or tectonic contacts. The group comprises rocks from two different basin cycles (*e.g.*, Kuchenbecker *et al.* 2015). The first one, a Tonian aborted rift basin, has been recorded within the studied area by the Capelinha Formation, which bounds the batholith to the South and presents quartzites, mica-schists, and meta-basalts (Castro 2014). The second basin cycle took place in the Cryogenian and marked the onset of a complete Wilson cycle, with the evolution of a rift basin to a passive margin setting. In the studied area, this rift stage is recorded by glacial meta-diamictites, quartzites, and schists from Chapada Acauã Formation, which are in contact with the batholith to the North. This unit comprises an individualized member, the Rio Preto Member, which is composed of metabasaltic schists (Gradim *et al.* 2005) that bound the RIB to the West. On the other hand, the passive margin stage is recorded by the Ribeirão da Folha Formation, the series of schists that occur in the Northeastern limit of the batholith.

METHODOLOGY

In order to reassess the cartography of the RIB, we acquired new field data and compiled the available geological maps and explanatory notes (Grossi-Sad *et al.* 1997b, Souza e Grossi-Sad 1997).

The geophysical data used were provided by Companhia de Desenvolvimento de Minas Gerais (CODEMIG) and are part of two different surveys from the Minas Gerais State Airborne

Geophysics Program — 2001 and 2008/2009. The area of the RIB is included in surveys 3 (Morro do Pilar — Serro — Guanhães) and 11a (Jaíba — Montes Claros — Bocaiúva) of this program. Survey 3 was performed by Megafísica (2001) and 11a, by Lasa (2009), following the parameters showed in Table 1.

The Anomalous Magnetic Field map, Analytical Signal Amplitude (ASA) map, Gamma Spectrometry map for each radioactive element (K, Th and U), and Ternary RGB image (R-K, G-eTh, B-eU) were generated using Oasis Montaj software (GEOSOFT), following the procedures listed in Figure 2.

Gamma spectrometry data were interpolated using the minimum curvature method (*e.g.*, Briggs 1974), and magnetometry data were interpolated by the bi-directional algorithm (GEOSOFT 2011). The gridding cell size used was 125 m, ¼ of the larger flight line spacing. The magnetometry data available were originally corrected for the International Geomagnetic Reference Field (IGRF) and diurnal variation. In addition, the directional cosine filter was applied in the N30W direction, and the Butterworth low-pass filter (500 m) was used for surveys 3 and 11a. For the gamma-spectrometry data, the filters were applied only for survey 3, because the images for this survey needed treatment in order to produce a better knitting with survey 11a. Thus, the Hanning filter was applied three times, followed by the Trend filter and the directional cosine in the N30W direction with grade 0.5. The filters applied were for eliminating tendencies from the flight line direction and for neutralizing ambient noises in the data.

RESULTS

Geological data

We described 165 outcrops along the entire area in order to determine the batholith area extent and to characterize the rocks present in both RIB and its surrounding units. Field data and outcrop location are shown in the Supplementary Data.

Table 1. Flight parameters for airborne geophysical data acquisition.

Parameter	Survey 3	Survey 11a
Flight line direction	N30W	N25W
Flight line spacing	250 m	500 m
Control line direction	N60E	N65E
Control line spacing	2.5 km	10 km
Interval between consecutive geophysical measurements	Magnetometer 0.1 s Spectrometer 1.0 s	Magnetometer 0.1 s Spectrometer 1.0 s
Average flight height	100 m	100 m
Approximate flight speed	200 km/h	273 km/h

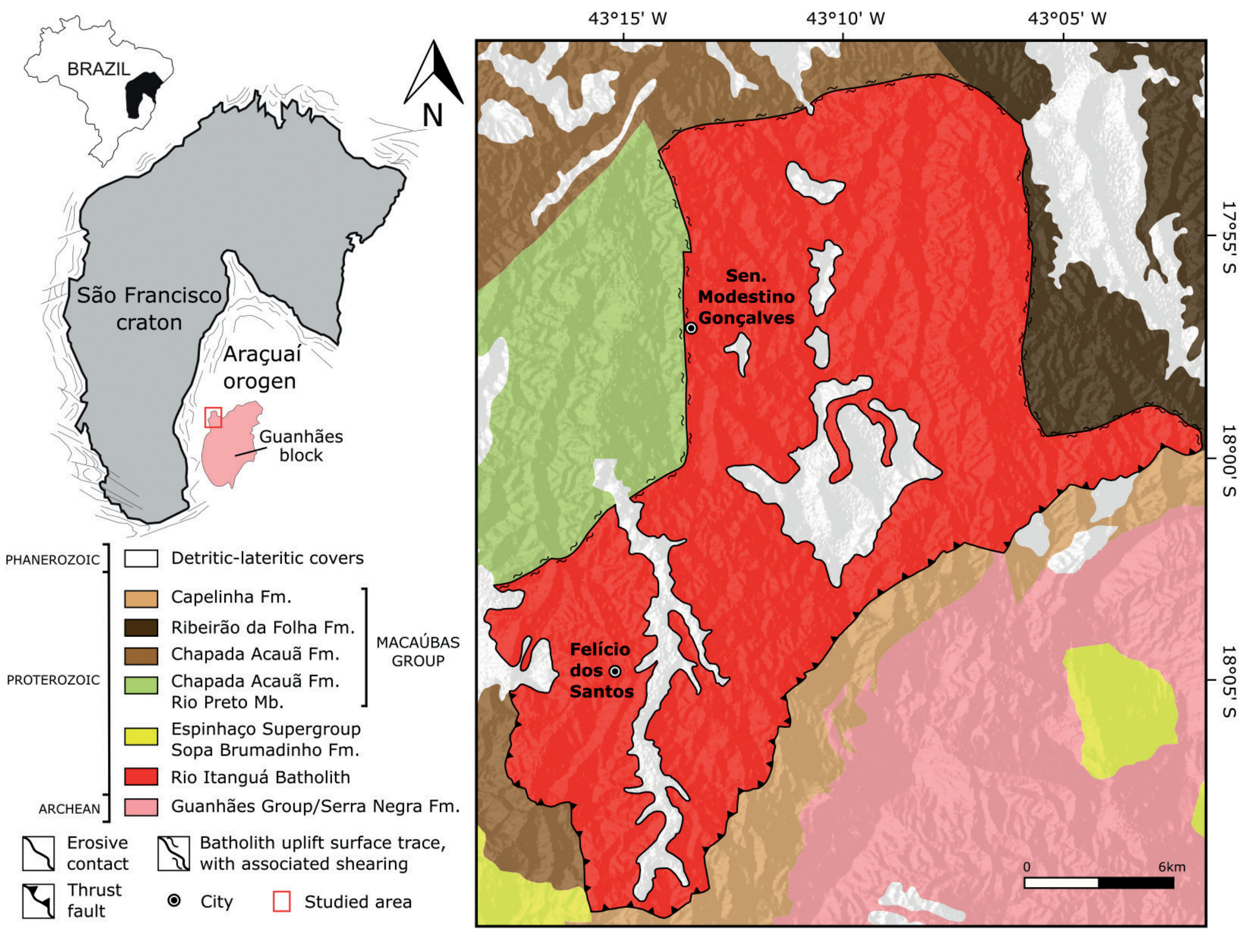

Figure 1. Location of Rio Itanguá Batholith in the Araçuaí orogen within the Guanhães block. The amplified figure from the studied area was adapted from Grossi-Sad *et al.* (1997b) and Souza & Grossi-Sad (1997), according to Pinto & Silva (2014).

In general, the granites described in the field occur in grey, rounded surface outcrops and are composed by quartz, feldspar, biotite, and muscovite. Some portions are highly affected by an anastomosing foliation that indicates shearing, whilst other portions are banded. Petrographically, it was possible to distinguish two different units in the RIB that are also recognizable in the gamma-ray spectrometry images (Fig. 3).

Unit A occurs in the Northern portion of the RIB and is composed by leucocratic granites that occur in two main facies: equigranular and porphyritic. Both facies are mainly formed by quartz, plagioclase, k-feldspar, biotite, and muscovite. The most common accessories are zircon, titanite, epidote (*stricto sensu*, clinozoisite and allanite), apatite, carbonate, rutile, and opaques. The porphyritic facies are characterized by feldspar phenocrysts, both plagioclase and k-feldspar, the latter usually bigger than the former (Fig. 3).

Unit B, located in the Southwestern part of the RIB, is composed by mesocratic granodiorite, and its mineralogy is mainly quartz, plagioclase, biotite and epidote, with the same accessories as Unit A. As a distinctive feature, Unit B does not show muscovite, exhibits a very low content of k-feldspar and its biotite and epidote (s. s.) content is higher than that of Unit A.

The rocks that surround the RIB are both metasedimentary and metaigneous (Fig. 4A-F). To the West, the RIB is bounded by the metabasaltic schists of Rio Preto Member (Lower Chapada Acauã Fm.; Fig. 4C), which are often strongly weathered. To the North, the limit of the RIB is made by schists, quartzites and metadiamictites — with granule to boulder sized clasts of quartzite, quartz and granite, in sandy matrix — from the Lower Chapada Acauã Formation (Fig 4D). To the Northeast, the RIB is limited by the micaschists from Ribeirão da Folha Formation, but the contact is mostly hidden under Cenozoic covers (Fig. 5). Along its Southeastern border, the RIB is bounded by Capelinha Formation, which is mainly composed of reddish mica schists with variable amounts of quartz and locally with quartzite lenses (Figs. 4E and 4F).

There is a plateau in the central portion of the RIB, in whose gentle slopes we identified several outcrops of mica schists quite similar to those present both in Capelinha and Ribeirão da Folha Formation. The schists (Fig. 4B) are strongly weathered and fresh outcrops are rare. In thin section, the rocks show lepidoblastic texture and are composed of alternated layers of micas (biotite + muscovite) and quartz, with anastomosing foliation and crenulation.

In the Southern part of the RIB, there are several outcrops of a metagabbro (Fig. 4A), whose locations align in a NW trend (Fig. 5). These rocks are composed mostly by fine crystals of amphibole and quartz, which are alternated in layers parallel to the foliation and deformed to a sigmoidal shape.

Covering all the above-mentioned units, there are thick layers of eluvial and colluvial lateritic soils. This unit covers schists on the central plateau, where it hosts a supergenic manganese deposit that is mined by Pedra Menina Company.

Gamma-ray spectrometry

Gamma-ray spectrometry data allow the distinction of two different rock units in the RIB, which show correspondence with its observed petrographic features. Furthermore, the radiometric signatures allowed an accurate delineation of the batholith and surrounding rock units in the geological map. To do so, we analyzed the K, U and Th channels separately and attributed values in a relative scale, ranging from low to high, as shown in Table 2. The ternary image composite of these three channels provided us the radiometric responses for the main geological units of the area.

Rio Itanguá Batholith: Unit A

Unit A, identified in the field as a leucocratic granite, outcrops in the Central, East and North portions of the batholith. It presents high to intermediate values of K, high Th, and

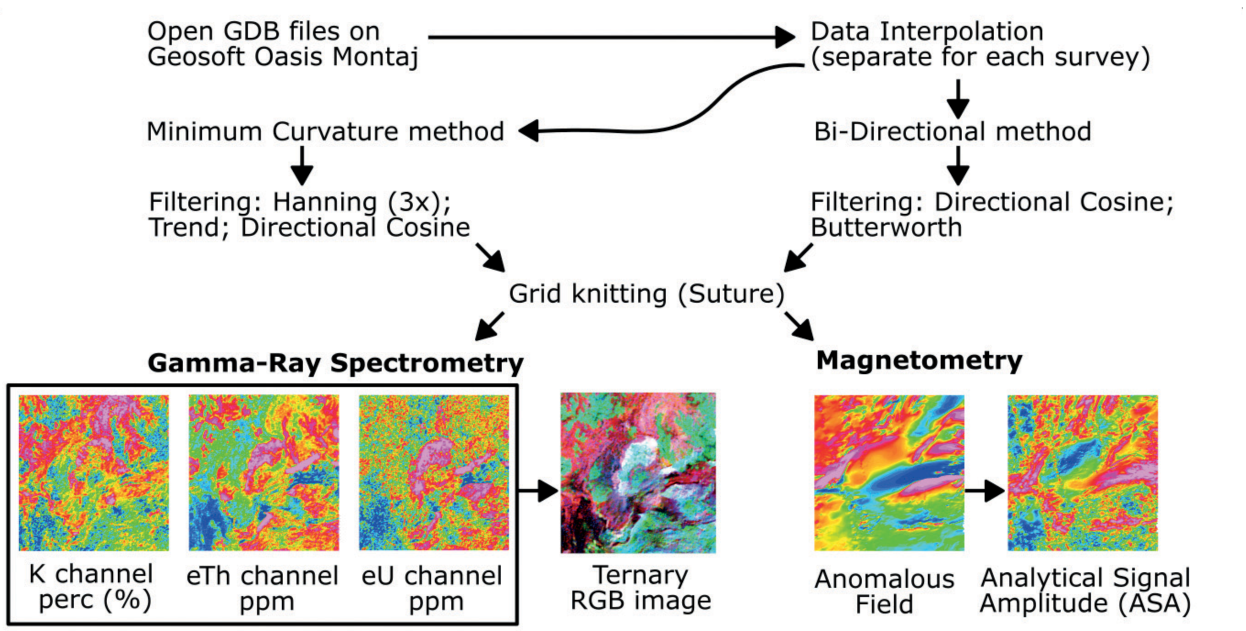

Figure 2. Flowchart of geophysical data processing for magnetometric and gamma-ray spectrometric images made on Geosoft Oasis Montaj.

high U. On the ternary RGB diagram, these values translate into a light, cyan colored area (Fig. 6). A patent characteristic revealed in the ternary RGB diagram is a pink halo around Unit A. It presents higher values of K and U and intermediate values of Th, which is different from the rest of the area covered by Unit A.

Rio Itanguá Batholith: Unit B

Unit B is a mesocratic granodiorite that outcrops in the Southwestern portion of the batholith and is characterized by intermediate K values, low Th, and intermediate to low U. On the ternary RGB image, these values are represented by a purple to pink area, contrasting with the response of Unit A.

Rio Preto Member — Lower Chapada Acauã Formation: Macaúbas Group

The rocks of this unit are green schists derived from a mafic volcanic protolith, unlike the other units of Macaúbas Group, which are derived from sedimentary protoliths. Thus, its radiometric signature is quite different from the other rocks, and this shows in the ternary RGB image — the blue area to the West of the batholith corresponds to these schists. They exhibit low to intermediate K, low Th, and intermediate U.

Chapada Acauã Formation: Macaúbas Group

The quartzites and schists of this unit crop out in the Northwestern part of the studied area and exhibit high K, low

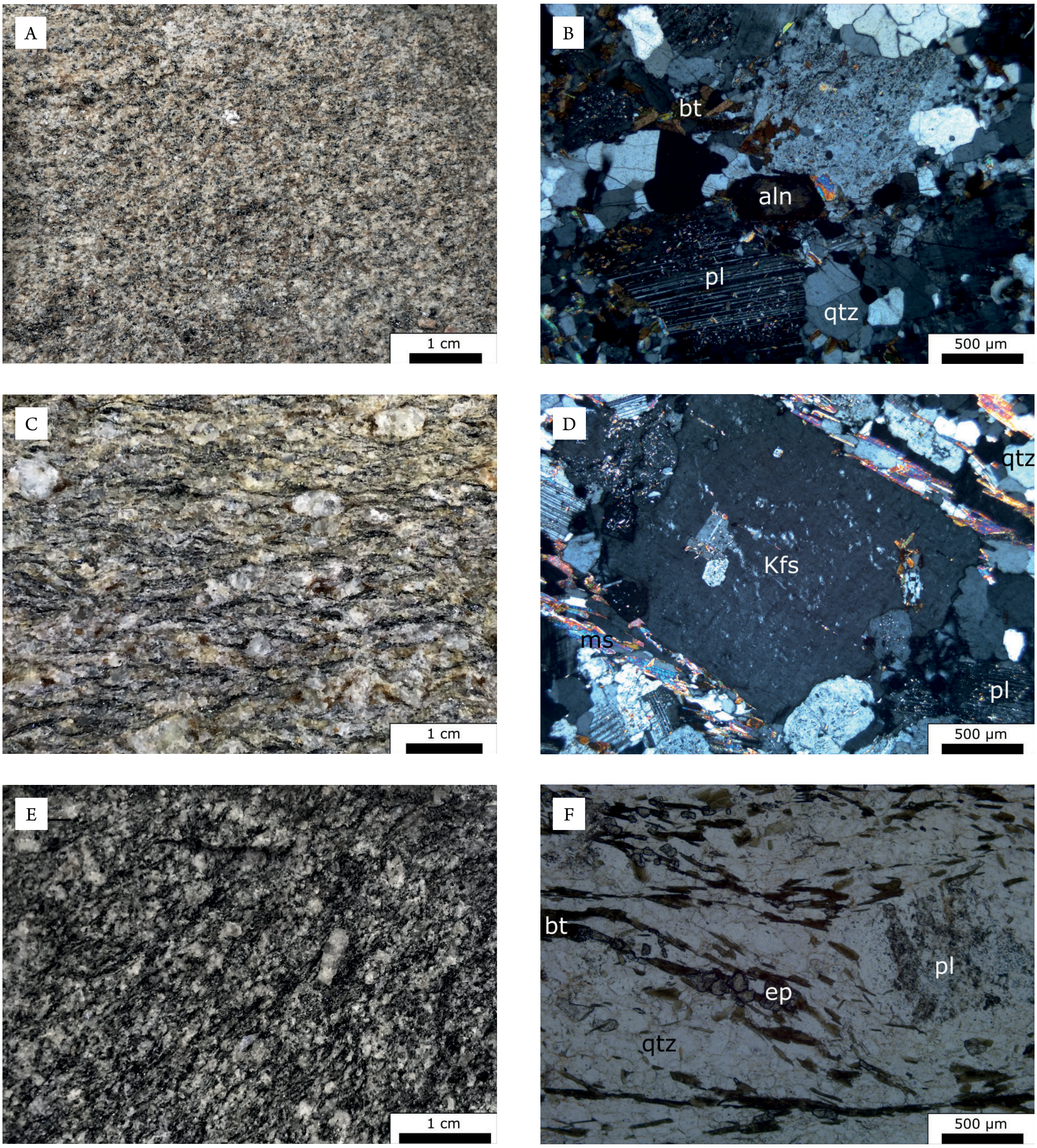

Figure 3. Macro- and micro-photographs of the Rio Itanguá Batholith (RIB) facies (mineral abbreviations according to Siivola & Schmid, 2007). (A) and (B) Unit A equigranular; (C) and (D) Unit A porphyritic; (E) and (F) Unit B.

Th and intermediate to high U responses. The ternary RGB image shows this area in a light pink coloring.

Ribeirão da Folha Formation: Macaúbas Group

The rocks of this unit are mainly mica-schists that outcrop at the Northeastern part of the studied area. They present high K, intermediate Th, and intermediate to high U. When seen in the ternary RGB image, it presents a shade of pink lighter than the response from Chapada Acauã Fm.

Capelinha Formation: Macaúbas Group

The quartzites and schists of this unit outcrop to the South of the RIB and generate the following radiometric responses: high to intermediate K, low Th, and low to intermediate U. In the ternary RGB image, its signature has a pink/purple color. Schists that occur in the gentle slopes of the plateau at the central portion of the area show the same radiometric features, which support the interpretation that they are included in Capelinha Formation.

Cenozoic covers

The Cenozoic covers found in the area present low values of K, intermediate values of U, and high Th. The high concentration of Th can be explained by its immobility during weathering processes. These values, when combined in a ternary RGB image, result in green areas that are distinct from all other signatures of units.

Figure 4. Units from the Rio Itanguá Batholith (RIB) area. (A) Foliated metagabbro with alteration crust; (B) micaschist from Capelinha Formation that outcrops in the central plateau; (C) dark grey phyllite from Rio Preto Member, Chapada Acauã Formation; (D) metadiamictite with boulder-sized clast of granite in a sandy matrix, Chapada Acauã Formation; (E) and (F) foliated quartzites from Capelinha Formation, southern border of RIB.

Magnetometry

The anomalous magnetic field map (IGRF-removed) was applied to obtain the analytical signal amplitude (ASA) map, where it was possible to identify a central domain that exhibits low analytical signal amplitude (Fig. 7). These lower values performed an oval-shaped area elongated at the NE-SW trend. In the map, this area represents the RIB and the mafic schists of Rio Preto Member.

Encircling this low amplitude area, there are contrasting high amplitude values that correspond to the surrounding Macaúbas Group schists and quartzites. These positive values are generically aligned in the NE-SW direction, which is the same direction as the granitic body and most of its boundaries.

Linear-shaped anomalies with high values of analytical signal amplitude at the NNW-SSE direction are also present. These anomalies correspond to meta-basic dikes that are exposed at the RIB area and covered by Macaúbas Group rocks.

DISCUSSION

As the gamma-ray spectrometry is the expression of the radiation near the surface (Ribeiro *et al.* 2013, Wilford *et al.* 1997), we could use the radiometric response identified as being from the batholith rocks to assess its map limits, if properly endorsed by the distribution of granite outcrops in the

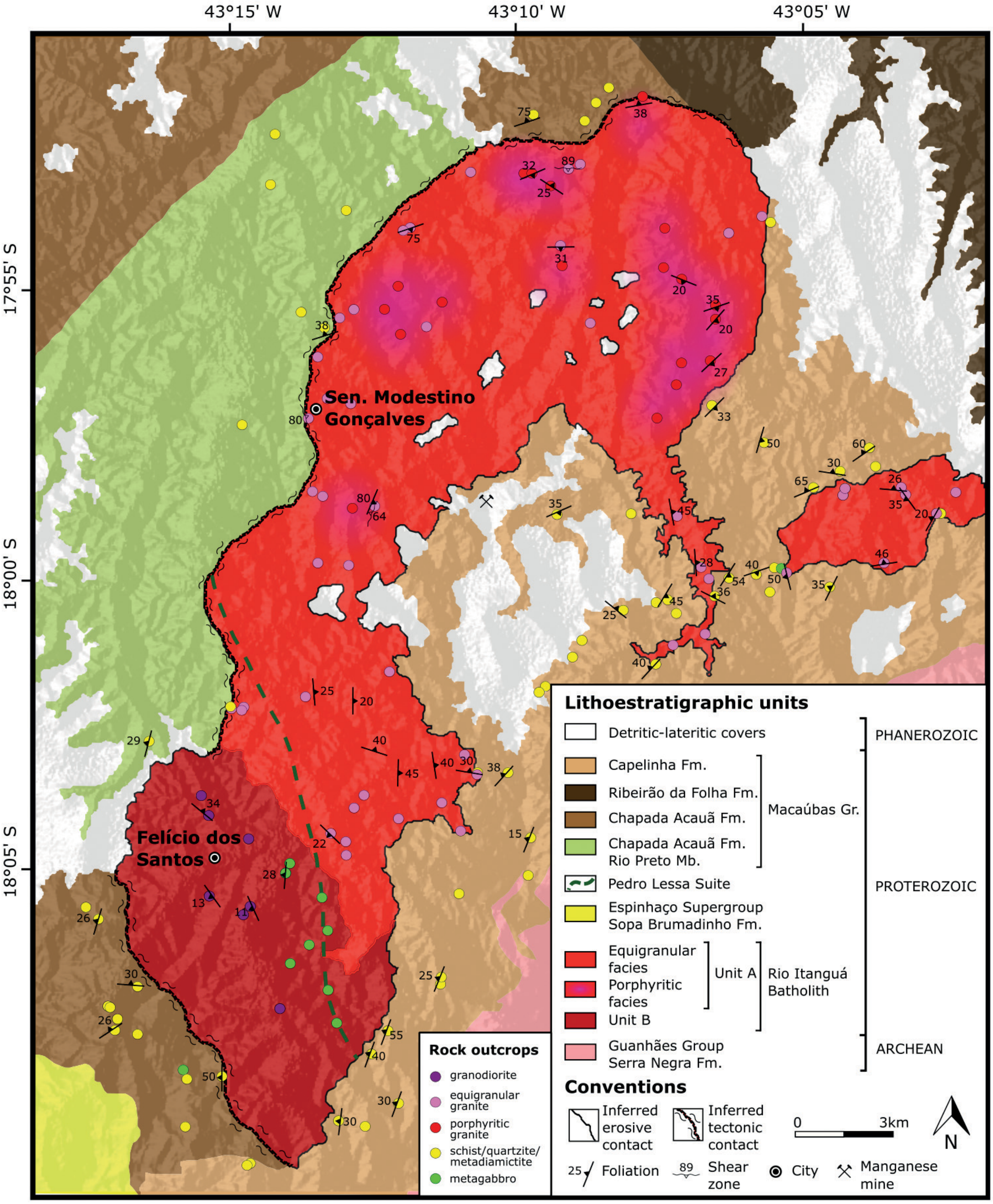

Figure 5. Geological map of the Rio Itanguá Batholith (RIB) made after compilation of new field data and geophysical analysis.

Table 2. Gamma-ray spectrometric responses for each unit present in the Rio Itanguá Batholith surrounding area.

Lithology	Stratigraphic Unit	Response in K channel	Response in Th channel	Response in U channel
Granite	Unit A (RIB)	High/ Intermediate	High	High
Granodiorite	Unit B (RIB)	Intermediate	Low	Intermediate/ Low
Green schist	Chapada Acauã Formation Rio Preto Mb.	Low/ Intermediate	Low	Intermediate
Schist/ Quartzite/ Metadiamictite	Chapada Acauã Formation	High	Low	Intermediate
Schist	Ribeirão da Folha Formation	High	Intermediate	Intermediate/ High
Quartzite/ Schist	Capelinha Formation	High/ Intermediate	Low	Low/ Intermediate
Detritic-lateritic Cover	Cenozoic Cover	Low	High	Intermediate

RIB: Rio Itanguá Batholith.

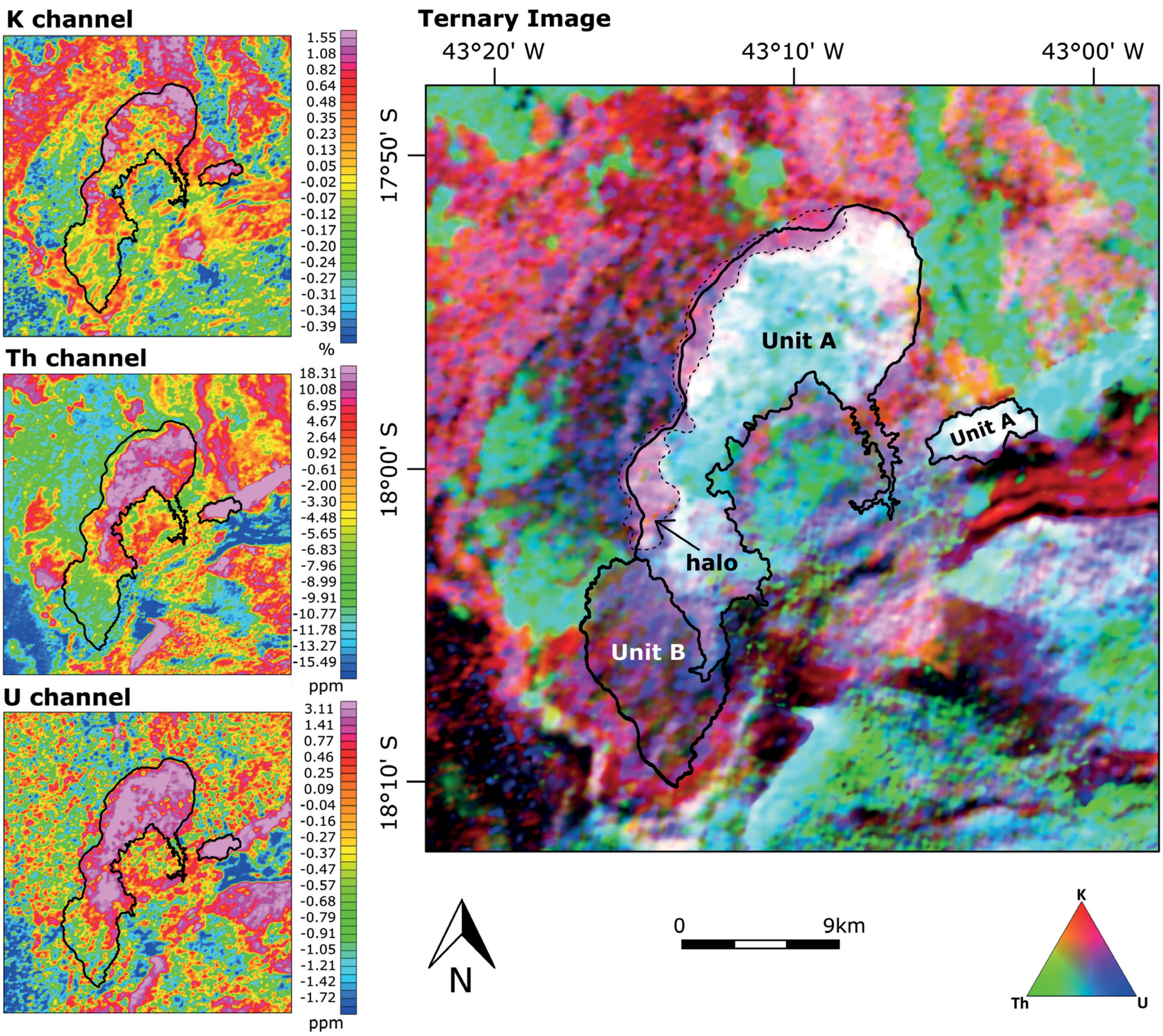

Figure 6. Gamma-ray spectrometry products obtained in the Rio Itanguá Batholith (RIB) area: K, Th and U channels and ternary composite RGB image showing RIB's limits and internal unit division. Highlighted by the dashed line is the pink halo to the North/ Northwest of the batholith.

field. By doing so, the batholith area changed from approximately 445 to 285 km² — reduction of 36% — with substantial changes made in the Central, Northern, Western, and Southern sectors (Fig. 8).

Some changes in the contact between the RIB and its surrounding units were proposed. In its Southwestern border, the gamma-spectrometric signature, alongside with the finding of quartzite outcrops, enlarged the area occupied by Chapada Acauã Formation. In the Northwestern sector, the contact between RIB and Rio Preto Member was refined based on their contrasting gamma-spectrometric responses.

Nevertheless, the most significant change was made in the central area, where mica-schists that were not previously mapped occur in the slopes of the central *plateau* and extend to the South and East. The schists occur on the RIB rocks as erosive remnants, which are a feature briefly mentioned by Grossi-Sad *et al.* (1997b), but that was not represented in the geological map made in the occasion. Despite the similarities in petrography to both Capelinha and Ribeirão da Folha schists, their gamma-ray spectrometric signature shows a better compatibility with Capelinha Formation; therefore, they

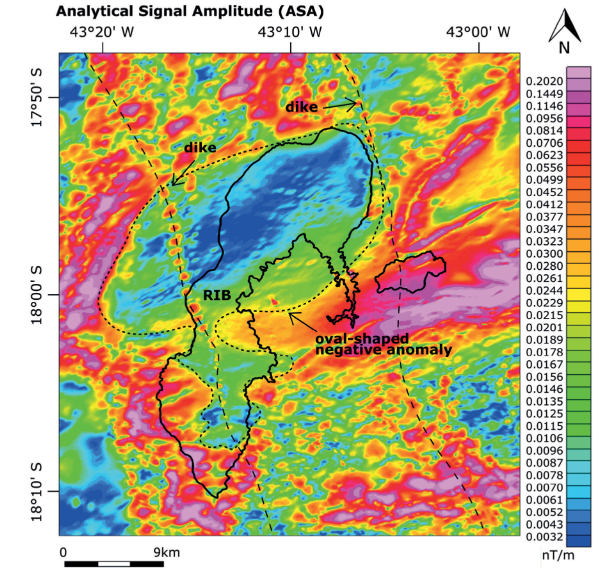

Figure 7. Analytical signal amplitude map, showing oval-shaped negative anomaly in the Rio Itanguá Batholith (RIB) outcropping area (surrounded by small dashes) and linear anomalies attributed to mafic dikes (larger dashes).

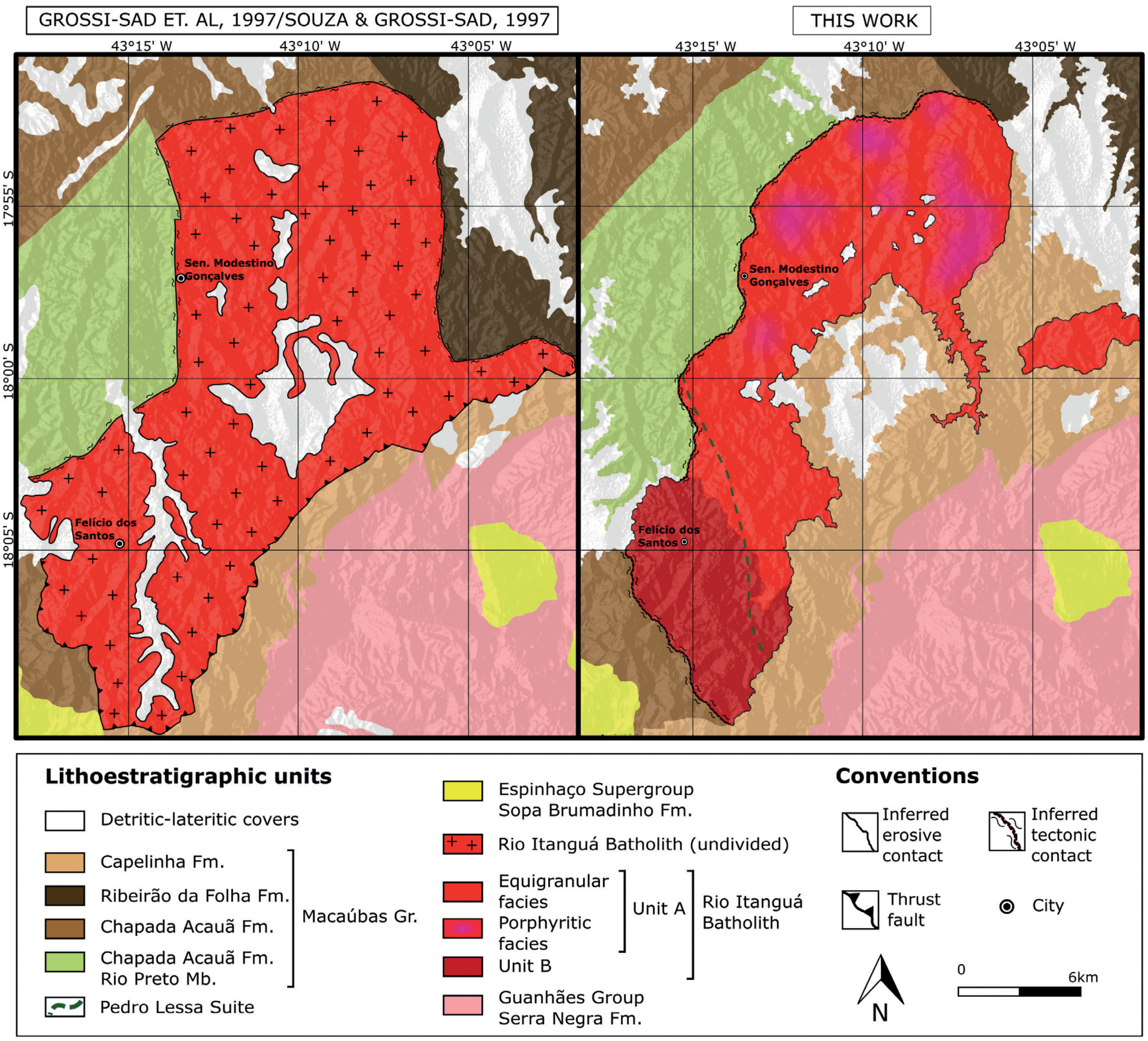

Figure 8. Comparison between Rio Itanguá Batholith map made at Espinhaço Project (Grossi-Sad *et al.* 1997b; Souza & Grossi-Sad 1997) and the resulting map of this work.

were tentatively included in this formation. Despite the lack of a clear gamma-spectrometric signature, the mapping of RIB in the Itanguá river valley, in the Eastern flank of the plateau, was justified by the presence of several granite outcrops along it.

Within the RIB itself, gamma-spectrometric data (K, U, and Th channels) show contrasting anomalies between the Northern and Southwestern parts of the batholith, following the petrographic division of RIB into two units (A - leucocratic granite; B - mesocratic granodiorite). However, the data are insufficient to observe if they are two facies from the same batholith, or if they are separate igneous bodies with different genesis and geological histories. If the later assumption prevails, we therefore suggest the Southern pluton to be named Felício, after the city of Felício dos Santos, and the Northern one, Mercês, after the former name of Senador Modestino Gonçalves, Mercês de Diamantina.

The magnetometry data shed light on the batholith expression at a greater depth, in contrast with the gamma-ray spectrometry data. The area of the RIB, in the ASA map, corresponds to an oval-shaped negative anomaly, which is somehow similar to what a pluton would look like seen from above. This distinct feature was interpreted as being the expression of the RIB in depth, which seems to extend further below the metabasaltic schists of Rio Preto Member (Lower Chapada Acauã Formation).

Based on magnetometry data, the mafic rocks found in the field were interpreted as a dike that crosses the RIB in the NW direction. There is no piece of evidence of these dikes cutting through the Macaúbas Group rocks around the batholith; thus, they were attributed to Pedro Lessa Suite, a mafic dike swarm abundant in the Southern Espinhaço range, which shows ages between 906 and 933 Ma (Dussin & Chemale Jr. 2012, Machado *et al*. 1989), older than the Macaúbas Group rocks.

The gamma-ray spectrometric data showed different radiometric patterns for each rock unit cropping out in the study area. This is an expected result, considering they have different compositions in terms of K, Th, and U. Dickson & Scott (1997) showed that the amount of these elements in the rock unit varies according to its content in SiO_2, the most acidic rocks having the higher content in the three elements. The element K, present primarily in K-feldspars, micas and clay minerals, is abundant in felsic igneous and metasedimentary rocks, but it is deficient in rocks derived from a mafic protholith, as appointed by Ulbrich *et al*. (2009). This explains the concentrations of this element in the RIB granites and Macaúbas metasedimentary rocks. The element K abundance on Unit A is much higher than on Unit B, due to the presence of K-feldspars in Unit A, while Unit B feldspars are mostly plagioclase, therefore their radiometric signature is contrasting. Th and U are common in accessory minerals such as allanite, xenotime, monazite and zircon, which are present in a variety of igneous and metamorphic rocks (Dickson & Scott 1997), including the two units that compose RIB.

The radiometric signature of the detrital-lateritic covers, like the ones in the Center, Northeast, North and West of the batholith, are noteworthy. They show a relative concentration of Th and a depletion in K, a result that usually comes from the immobility of Th during the weathering processes, as contrasted with the mobility of K, due to its solubility in aqueous solutions (Ulbrich *et al*. 2009, Wilford *et al*. 1997).

The halo observed around the Unit A of RIB presents high K and lower Th when compared to the other parts of the granitic body. Two hypotheses can explain this fact: either the leaching of K in the vicinity led to an accumulation of this element on the borders of the plutonic body due to lower topography, or there was a concentration of this element by metasomatism on the RIB borders, at the time of pluton intrusion or by subsequent fluid percolation. The boundary between RIB and Chapada Acauã Formation is marked by faults that could favor the activity of either of these processes.

Some of our results raise interesting questions about the structural evolution of the area. For example, in the Espinhaço Project, a strip of rocks from Capelinha Formation was mapped in tectonic contact with the RIB. However, the erosive remnants of the schist identified in the central plateau have geographic continuity in this unit, which led us to reinterpret this boundary as erosive. The other RIB boundaries were interpreted as tectonic, in agreement with the previous maps. The nature of these boundaries, however, deserves to be further investigated in future works, allowing an understanding of the structural behavior of the RIB during Neo-Proterozoic orogenesis.

CONCLUSION

The techniques used in this study allowed the reevaluation of the geologic cartography of RIB. Based on the obtained results, we defined a new contour for the batholith and identified two distinct rock units that show petrographic and geophysical differences. We were also able to identify a dike and a huge area covered by schist, two features that were not present in the previous maps.

The geophysical data proved to be important tools for the geological mapping, and the substantial data obtained in the analysis of this tiny area indicates the importance of re-evaluating older geological maps, taking the now available magnetometry and gamma-ray spectrometry data into account.

ACKNOWLEDGMENTS

The authors would like to thank CODEMIG for providing the aerogeophysical data, Conselho Nacional de Desenvolvimento da Pesquisa (CNPq) for the financial support to this research (Processes 09106/2017-6 and 405254/2016-4) and Centro de Estudos em Geociências/Instituto de Ciência e Tecnologia/Universidade Federal dos Vales do Jequitinhonha e Mucuri (UFVJM) for lab support. The first author would like to thank UFVJM for providing the master's degree scholarship.

ARTICLE INFORMATION
Manuscript ID: 20190019. Received on: 03/13/2019. Approved on: 06/26/2019.
J. G. performed geological mapping and geophysical analyses, wrote the draft of the manuscript and prepared the figures. M. K., D. B., and T. N. provided advisor regarding geological mapping and geophysics, and also improved the manuscript through corrections and suggestions.
Competing interests: The authors declare no competing interests.

REFERENCES

Alkmin, F.F. 2017. The Araçuaí Belt. *In*: Heilbron M., Cordani U.G., Alkmin F.F. (eds.), *São Francisco craton, eastern Brazil:* Tectonic genealogy of a miniature continent. Switzerland, Springer, p. 255-276.

Almeida F.F.M. 1977. O Cráton do São Francisco. *Revista Brasileira de Geociências*, **7**(4):349-364.

Amaral W.F., Santos T.J.S. 2008. Airborne geophysical and tectonics of the Ceará central domain, eastern region of the Santa Quitéria magmatic arc, Borborema province, NE Brazil. *Revista Brasileira de Geofísica*, **26**(4):527-542. http://dx.doi.org/10.1590/S0102-261X2008000400012

Barbuena D., Souza Filho C.R., Leite E.P., Miguel JR. E., Assis R.R., Xavier R.P., Ferreira F.J.F., Barros A.J.P. 2013. Airborne geophysical data analysis applied to geological interpretation in the Alta Floresta Gold Province, MT. *Revista Brasileira de Geofísica*, **31**(1):169-186. http://dx.doi.org/10.22564/rbgf.v31i1.254

Briggs I.C. 1974. Machine contouring using minimum curvature. *Geophysics*, **39**(1):39-48. https://doi.org/10.1190/1.1440410

Brito Neves B.B., Kawashita K., Cordani U.G., Delhal J. 1979. A evolução geocronológica da Cordilheira do Espinhaço: dados novos e integração. *Revista Brasileira de Geociências*, **9**(1):71-85.

Castro M.P. 2014. *Caracterização geológica da Formação Capelinha como uma Unidade Basal do Grupo Macaúbas em sua Área Tipo, Minas Gerais*. MS Dissertation on Crustal Evolution and Natural Resources, Escola de Minas, Universidade Federal de Ouro Preto, Ouro Preto, 114 p.

Cuvier G., Brongniart A. 1811. *Essai sur la Géographie Minéralogique des Environs de Paris, avec une Carte Géognostique, et des Coupes de Terrain*. Paris, Baudouin, 278 p.

Dickson B.L., Scott K.M. 1997. Interpretation of aerial gamma-ray surveys – adding the geochemical factors. *AGSO Journal of Australian Geology & Geophysics*, **17**(2):187-200.

Dussin I.A., Chemale Jr. F. 2012. *Geologia estrutural e estratigrafia do sistema Espinhaço–Chapada Diamantina e sua aplicação nas bacias mesozóico-cenózoicas da margem passiva brasileira*. Rio de Janeiro, Petrobras, 218 p.

GEOSOFT. 2011. *Mapping and Processing System – The core software platform for working with large volume spatial data*. Quick StartTM Tutorials. Available on: <https://pt.scribd.com/doc/187939564/Oasis-Montaj-Tutorial-English>. Accessed on: Aug. 14, 2019.

Gorlt G. 1972. Fazieswechsel und Metamorphose in der weslichen Serra Negra (Espinhaço Zone, Minas Gerais, Brasilien). *Geologische Rundschau*, **61**:166-201.

Gradim R.J., Alkmin F.F., Pedrosa-Soares A.C., Babinski M., Noce C.M. 2005. Xistos verdes do Alto Araçuaí, Minas Gerais: vulcanismo básico do rifte neoproterozóico Macaúbas. *Revista Brasileira de Geociências*, **35**(4 Supl.):59-69.

Grossi-Sad J.H., Lobato L.M., Pedrosa-Soares A.C., Soares-Filho B.S. 1997a. *Projeto Espinhaço (textos, mapas e anexos)*. Belo Horizonte, COMIG. 1 CD-ROM.

Grossi-Sad J.H., Roque N.C., Knauer L.G., Noce C.M., Fonseca E. 1997b. Geologia da Folha Carbonita. *In*: Grossi-Sad J.H., Lobato L.M., Pedrosa-Soares A.C., Soares-Filho B.S. (eds.). *Projeto Espinhaço (textos, mapas e anexos)*. Belo Horizonte, COMIG, p. 1251-1371. 1 CD-ROM.

Hagedorn M.G. 2004. *Contexto geotectônico da Serra do Espinhaço e domínios adjacentes a leste (Minas Gerais) com ênfase em aspectos geoquímicos e geocronológicos*. PhD Thesis, Instituto de Geociências e Ciências Exatas, Universidade Estadual Paulista "Júlio de Mesquita Filho", 222 p.

Hettich M. 1973. *Zur Stratigraphie und Genese des Macaúbas nördlich der Serra Negra, Espinhaço - Zone (Minas Geraes, Brasilien)*. Master Dissertation, Freiburg University, Germany, 42 p.

Kuchenbecker M., Pedrosa-Soares A.C., Babinski M., Fanning M. 2015. Detrital zircon age patterns and provenance assessment for pre-glacial successions of the Neoproterozoic Macaúbas Group, Araçuaí orogeny, Brazil. *Precambrian Research*, **266**:12-26. http://dx.doi.org/10.1016/j.precamres.2015.04.016

Lasa Engenharia e Prospecções S.A. 2009. *Levantamento aerogeofísico de Minas Gerais, Área 11A:* Jaíba – Montes Claros – Bocaiúva. Relatório final do levantamento e processamento de dados magnetométricos e gamaespectrométricos. Texto técnico. Belo Horizonte. 271 p. v. 1.

Machado N., Schrank A., Abreu F.R., Knauer L. G., Almeida-Abreu P. A. 1989. Resultados preliminares da geocronologia U–Pb na Serra do Espinhaço Meridional. *Boletim do Núcleo Minas Gerais*, **10**:171-174.

Megafísica Survey Aerolevantamentos S.A. 2001. *Levantamento aerogeofísico de Minas Gerais, Área 3: Morro do Pilar – Serro – Guanhães*. Relatório final do levantamento e processamento de dados magnetométricos e gamaespectrométricos. Texto técnico. Belo Horizonte. 40 p. v. 1.

Moraes L.J. 1937. *Geologia Econômica do Norte de Minas Geraes*. Rio de Janeiro, Departamento Nacional de Produção Mineral, Serviço de Fomento à Produção Mineral, 191 p. v. 19.

Pedrosa-Soares A.C., Noce C.M., Alkmin F.F., Silva L.C., Babinski M., Cordani U., Castañeda C. 2007. Orógeno Araçuaí: Síntese do conhecimento 30 anos após Almeida 1977. *Geonomos*, **15**(1):1-16. https://doi.org/10.18285/geonomos.v15i1.103

Pinto C.P. & Silva M.A. 2014. *Geological map of the Minas Gerais state*. 1:1,000,000 scale. Belo Horizonte: CODEMIG/CPRM. Available in: <portalgeologia.com.br/index.php/mapa>. Accessed on: Feb. 19, 2017.

Portal da Geologia. Available at: <www.portalgeologia.com.br>. Accessed on: Feb. 16, 2019.

Rattenbury M.S., Cox S.C., Edbrooke S.W., Martin A.P. 2016. Integrating airborne geophysical data into new geological maps of New Zealand mineral provinces. *In*: Christie A.B. (ed.), *Mineral deposits of New Zealand:* exploration and research. Carlton: Australasian Institute of Mining and Metallurgy. Monograph series (Australasian Institute of Mining and Metallurgy), v. 31. p. 37-44.

Reis H.L.S., Barbosa M.S.C., Alkmin F.F., Pedrosa-Soares A.C. 2012. Magnetometric and gamma spectrometric expression of southwestern São Francisco Basin, Serra Selada quadrangle (1:100.000), Minas Gerais state. *Revista Brasileira de Geofísica*, **30**(4):445-458.

Ribeiro V.B., Mantovani M.S.M., Louro V.H.A. 2013. Aerogamaespectrometria e suas aplicações no mapeamento geológico. *TerræDidatica*, **10**(1):29-51.

Serviço Geológico do Brasil. Available at: <http://geobank.cprm.gov.br/>. Accessed on: Feb. 16, 2019.

Siivola J., Schmid R. 2007. *List of Mineral abbreviations*. IUGS Subcommission on the Systematics of Metamorphic Rocks, 14 p.

Smith W. 1815. *A geological map of England and Wales and part of Scotland:* London, British Geological Survey. 1 sheet.

Souza M.A.T.A., Grossi-Sad J.H. 1997. Geologia da Folha Rio Vermelho. *In*: Grossi-Sad J.H., Lobato L.M., Pedrosa-Soares A.C., Soares-Filho B.S. (eds.). *Projeto Espinhaço (textos, mapas e anexos)*. Belo Horizonte, COMIG, p. 1667-1806. 1 CD-ROM.

Toloczyki M. 1982. *Der Granitaufbruch von Senador Modestino Gonçalves und sein geologischer Rahmen (Präkambrium, Minas Gerais, Brasilien)*. Master Dissertation, Freiburg University, Germany, 76 p.

Ulbrich H.H.G.J., Ulbrich M.N.C., Ferreira F.J.F., Alves L.S., Guimarães G.B., Fruchting A. 2009. Gamma-spectrometric Surveys in Differentiated Granites. I: a Review of the Method, and of the Geochemical Behavior of K, Th and U. *Geologia USP Série Científica*, **9**(1):33-53.

Whitmeyer S.J., Nicoletti J., De Paor D.G. 2010. The digital revolution in geologic mapping. *GSA Today*, **20**(4):4-10. https://doi.org/10.1130/GSATG70A.1

Wilford J.R., Bierwirth P.N., Craig M.A. 1997. Application of airborne gamma-ray spectrometry in soil/regolith mapping and applied geomorphology. *AGSO Journal of Australian Geology & Geophysics*, **17**(2):201-216.